

FERMI NATIONAL
ACCELERATOR LABORATORY

SUMMER INTERNSHIP

FINAL REPORT

Study of cosmic ray background
for the SBN program detectors

Author:

Alessio GIARNETTI
giarnetti.alessio@gmail.com

Supervisor:

Anne SCHUKRAFT

October 13, 2018



Abstract

SBN program at Fermilab is an experiment that looks at short baseline neutrino oscillations. Three LAr-TPC detectors (SBND, MicroBooNE and Icarus) will be located along the BNB beam on the surface. Due to detector position the cosmic background is very important. For example, the first analysis for MicroBooNE, which is the only detector already working, shows that more than one third of the selected events are cosmic events. After Run 1 data taking, scintillator panels (CRT) have been installed around the detector so to tag cosmic particles.

In the analysis described here simulated CRT data have been implemented for the first time in the selection, so to understand how much they can help in background rejection.

A simple veto approach can improve the purity of the selection, but also reject many signal events. The best results can be obtained using only the cathode and top CRT panels.

Considering timing information, and requiring coincidence between the CRT hit time and the beam spill time, is possible to not reject any signal event, increasing the purity without losing efficiency.

Contents

1	Introduction	3
2	CRT veto	8
3	Recovery of lost events in flash matching	15
4	Time matching	16
5	CRT in future detectors	21
	Conclusion	22
	Appendix	23
	Bibliography	28

1 Introduction

Neutrino oscillations are one of the most important discovery in modern physics, since they implies that neutrinos have mass, even though for the Standard Model they are massless. The oscillation probability depend on the difference between the mass eigenvalues squared, the mixing angle, the distance traveled by the particle and the neutrino energy.

Short baseline accelerator experiments have shown recently an oscillation excess at low energy, where oscillations are not expected at all. This kind of anomaly is confirmed by reactor and gallium experiment. The excess can be explained introducing new physics, for example a sterile neutrino heavier than the others. The SBN program at Fermilab want to explore further short baseline neutrino oscillations [1]. The experiment consists in a muon neutrino beam (BNB) with a mean energy of 600MeV that pass through 3 Liquid Argon Time Projection Chamber detectors. The near detector is SBND and it is going to be built in the next years. It will be located 110m from the target. The second detector, the smallest one, is MicroBooNE [3] and is located 470m from the target. It is already taking data since 2015. The far detector is ICARUS, 600m from the target, and it is going to work soon.

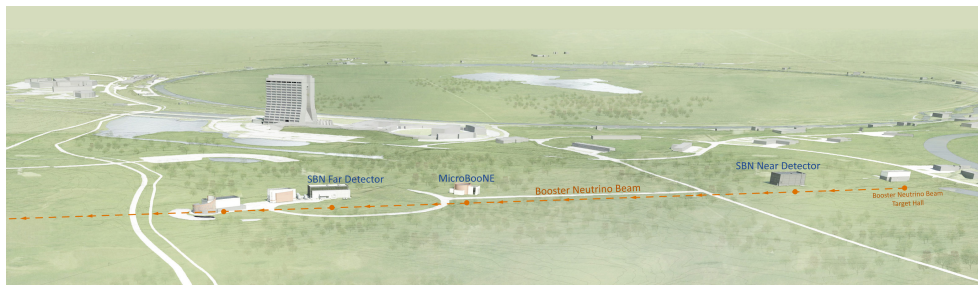


Figure 1: BNB beam and SBN detectors at Fermilab.

LAr-TPCs use three collection wires planes to reconstruct the particle tracks in 3 dimensions and they have a very good imaging capability. But they are also quite slow, because the ionized electrons take time to reach the wires, so the readout window is usually some milliseconds long.

For this reason, detectors, which are also on the surface, collect a lot of cosmic rays tracks. To give an example, only one each 700 triggered beam spills contain a neutrino vertex, and every neutrino event has 10-20

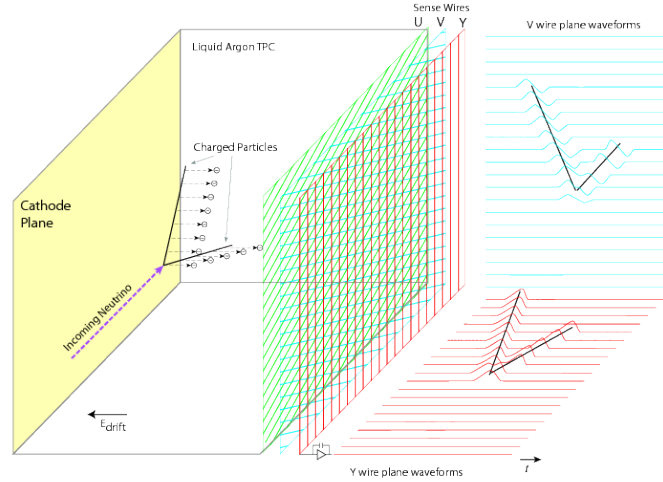


Figure 2: A LAr-TPC. A particle that enter in the detector can interact with the argon atoms and the ionized elections can drift to the anode because of the electric field. Three wire planes with three different orientations can be used for the track reconstruction.

overlying cosmic tracks. It is very important to develop a strategy to reduce this background. One of the first analysis that uses MicroBooNE data is the ν_{μ} CC inclusive cross section [4]. To search for a neutrino interaction it is necessary to find the muon track that comes from the vertex. This long muon track is very similar to the cosmic muons tracks, so a selection that try to choose the right particle has been developed. After all the cuts made for the CC inclusive, the selection has only 53.1% of purity and 55.3% of efficiency. Still the 36.8% of the selected events have cosmic origin.

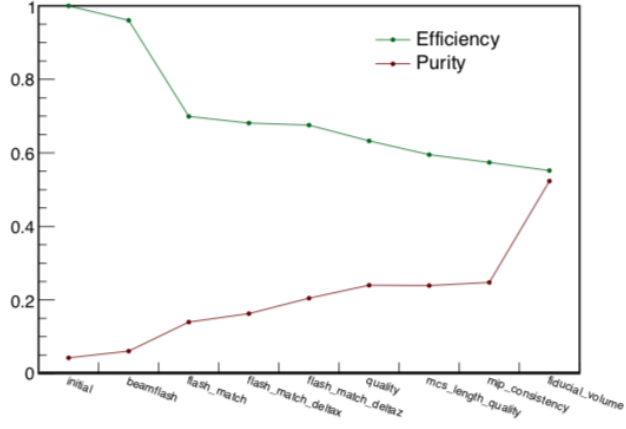


Figure 3: Efficiency and purity after every selection step.

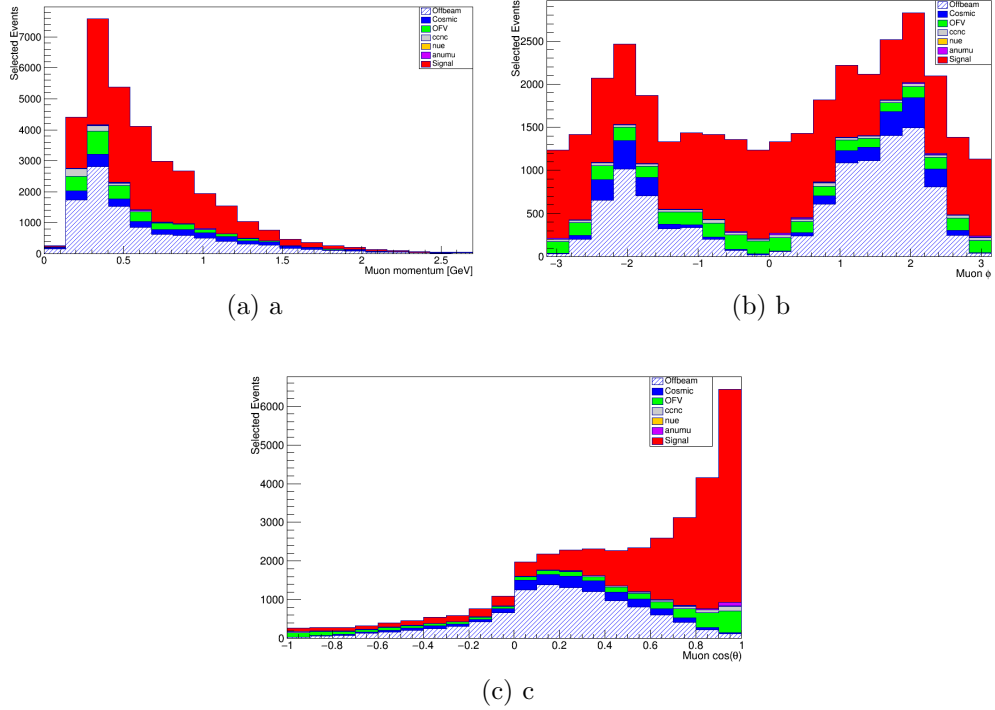


Figure 4: Number of events after the selection in function of Muon momentum (a), Muon ϕ (b) and Muon $\cos\theta$ (c).

Signal	53.1%
Cosmic	6.8%
OUTFV	8.1%
CCNC	1.7%
ν_e	0.08%
$\bar{\nu}_\mu$	0.5%
Off-beam	29.7%

Table 1: Event composition after selection. The purity of the signal is 53.3%, and it is clear that the main part of the background comes from cosmic events.

Usually there are two types of cosmic background:

- Offbeam, when the event contains no neutrino vertex.
- Cosmic, when the event contains a neutrino vertex but the selection choose the wrong muon track.

This two looks very similar in many features, so it is possible to reduce both with a good strategy.

In order to reduce the cosmic background, scintillator panels have been installed all around MicroBooNE cryostat. This system is called Cosmic Ray Tagger (CRT) [2]. Limited space in the detector building did not allow to have a full coverage.

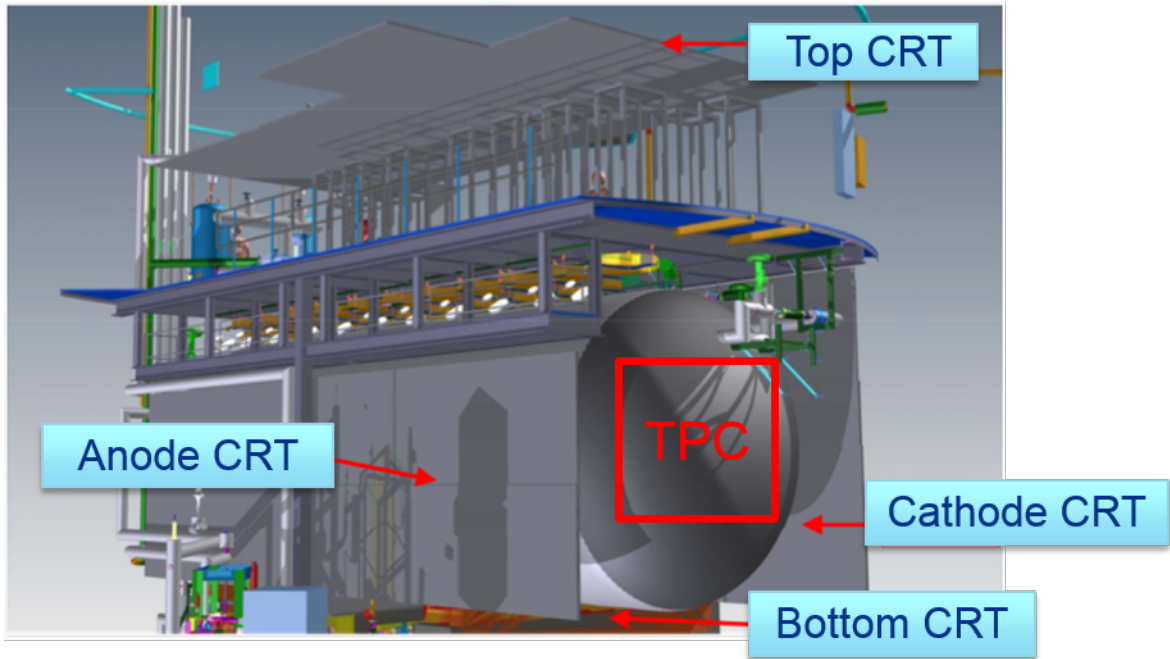


Figure 5: View of the CRT panels.

Since data used for the CC inclusive were taken before the CRT installation, the selection used only PMT and TPC information. This project was about implementing the CRT panels for the first time in the CC inclusive analysis, so to understand how much they could help in the background mitigation. The CRT consist in several panels, so to provide not only the arrival time but also the position of the hitting particle. To simplify the geometry CRT has been divided in only 6 big panels, one on the top, one on the anode side, two on the cathode side and two on the bottom.

2 CRT veto

To include CRT panels in the selection, was needed to describe them in the TPC coordinates. In this system z is the beam direction, y is perpendicular to the surface and x is the axis that goes from the anode to the cathode.

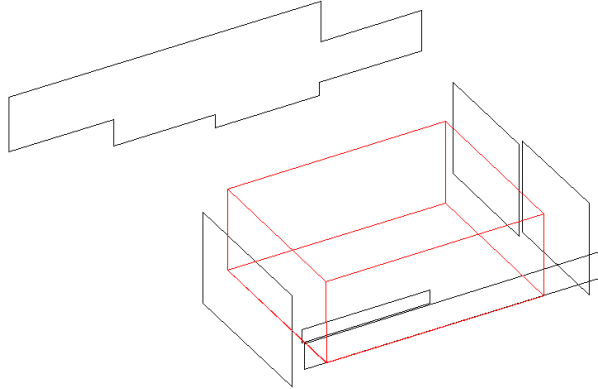


Figure 6: Position of the panels around the cryostat (in red). The one in the right is the cathode panel, the one on the left is the anode panel.

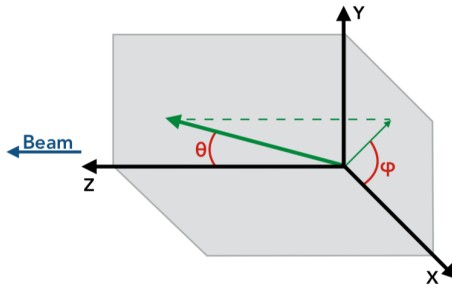


Figure 7: Angles definition in MicroBooNE.

In the first part of the analysis, two datasets have been used: On-beam simulated events and Off-beam data. In order to have the same amount of events from these two datasets, it was necessary to scale the off-beam considering the simulated POT. The factor scale used in this analysis was 0.707.

The simplest way to include the CRT in the event selection is using a veto. The idea of the CRT veto consist on rejecting all the selected muons that are hitting one of the panels. In order to extend the tracks that are inside the fiducial volume of the detector, two angles are needed. In particular, θ is the angle between the track and the beam axis, and ϕ is the angle on the x-y plane.

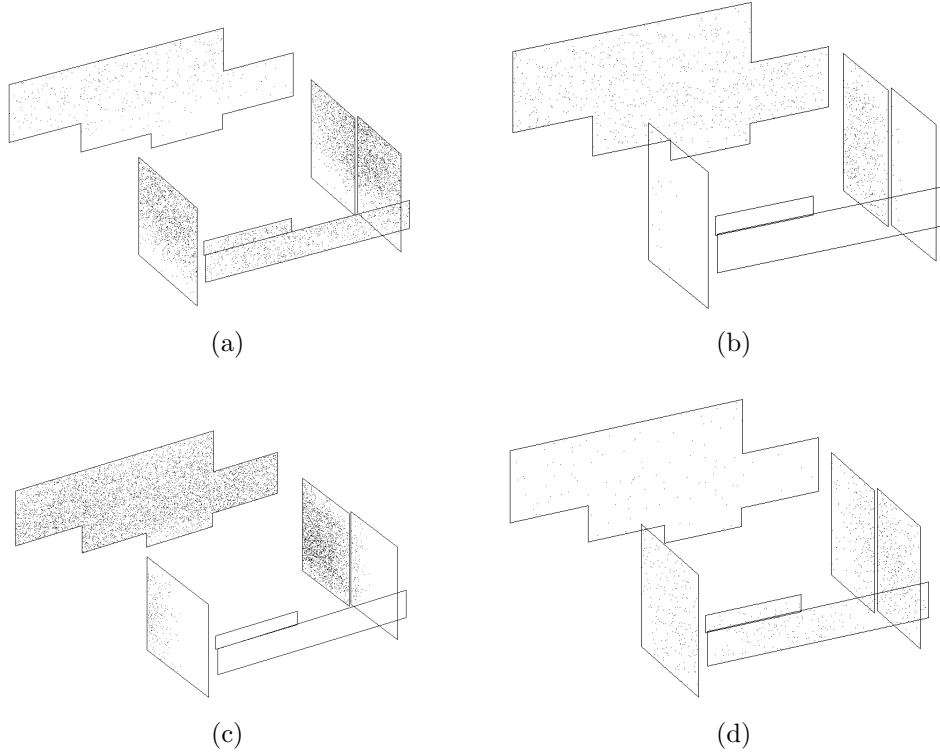


Figure 8: Intersection points of the tracks with the CRT panels for Signal (a), cosmic (b), off-beam (c) and OUTFV (d) events. The panels that are tagging the majority of the cosmic muons are the cathode and the top panels.

For the signal and the out of fiducial volume events, which are simulated, the true muon momentum is known, so it is possible to understand if the muons are stopping in the liquid Argon before reaching the panel [5]. Almost half of them are absorbed inside the cryostat.

For the cosmic data, it is not possible to know if the muons are reaching the panels while they are exiting the cryostat, since their true momentum

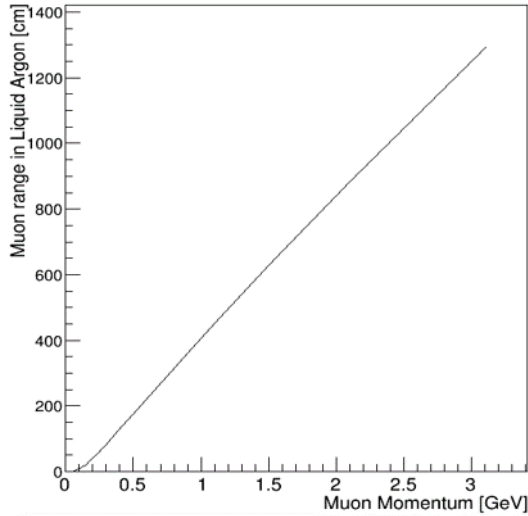


Figure 9: Muon range in Liquid Argon. Muons in MicroBooNE detector have can travel few meters.

is not known. So the cosmic muon tracks were extended only upwards, because it is sure that cosmic rays are entering in the TPC from above. For the Neutral current background and the ν_e background, the tracks were not extended at all because pions and electrons never exit the TPC.

Fig.8 shows where the tracks hit the panels, for cosmic, off-beam, out of fiducial volume (events in which the vertex is not in the fiducial volume) and signal events. The panels that help the most for the cosmic background rejection are the top and the cathode panles. This plot shows also a big asymmetry between the two side panels. The reasons for this asymmetry are the dimension of the anode panel, which is smaller than the cathode panel, and its position, since the cathode is much closer to the top, where the cosmic rays are coming from.

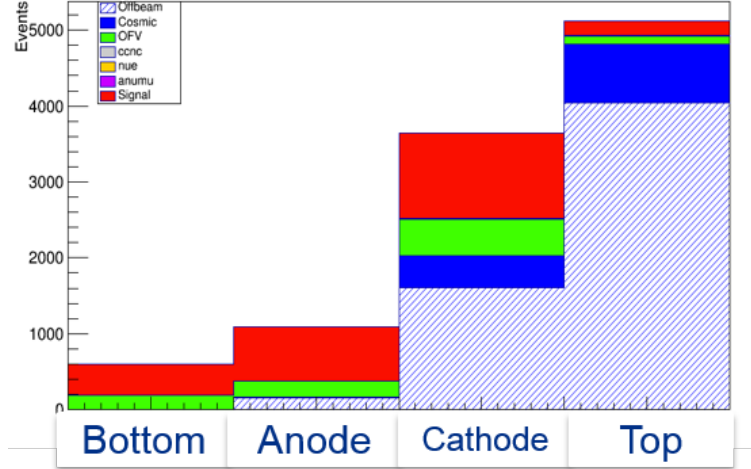


Figure 10: Number of tracks rejected by each panel. It's clear that the top panel is rejecting most of the cosmic background, because cosmic rays should come from the the top. There is also a big asymmetry between the anode and the cathode panel. The cathode is able to tag much more cosmic tracks, and this is because it is closer to the top, and it is bigger than the anode.

Fig.10 shows the number of tracks tagged by each panel. It is clear that is better to use only the cathode and the top panel, because the other two are basically rejecting only signal events, decreasing the efficiency. With this new stage of the selection, considering only the two useful panels, the purity can be improved of 12%, while the efficiency become 51%.

Signal	65.1%
Cosmic	4.1%
OUTFV	8.2%
CCNC	2.2%
ν_e	0.14%
$\bar{\nu}_\mu$	0.68%
Off-beam	19.2%

Table 2: Event composition after the CRT veto using only the top and the cathode panels. The purity of the signal is bigger than using the previous selection, and the cosmic background is reduced.

A good cut should let the efficiency be flat in function of the main variables. In this case, the efficiency after the CRT veto has the same shape of the previous selection. The only region where this new cut change the curve is from $\phi = -1$ to $\phi = 1$, where the cathode panel is rejecting some signal events.

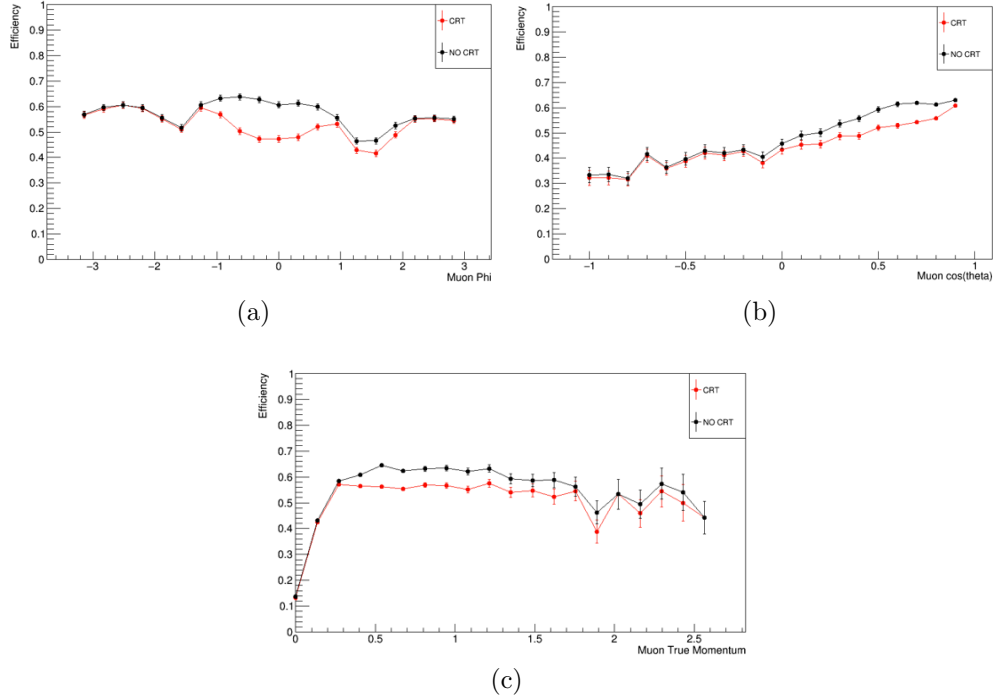


Figure 11: Efficiency in function of muon ϕ (a), muon $\cos\theta$ (b) and muon momentum (c). The black line is the efficiency of the previous selection, the red one is adding the CRT veto. The shape of the two lines is almost everywhere the same except for the ϕ region where the cathode panel is rejecting signal events.

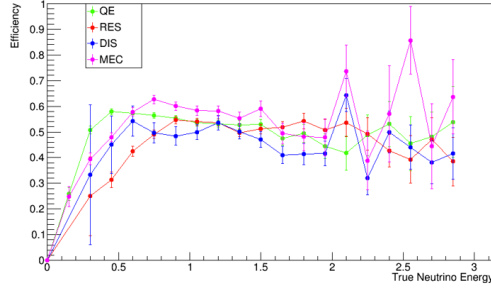


Figure 12: Efficiency of the CRT veto selection in function of the true neutrino energy considering the four main interaction modes: Quasi-Elastic (QE), Meson Exchange Current (MEC), Deep Inelastic Scattering (DIS) and Resonant (RES).

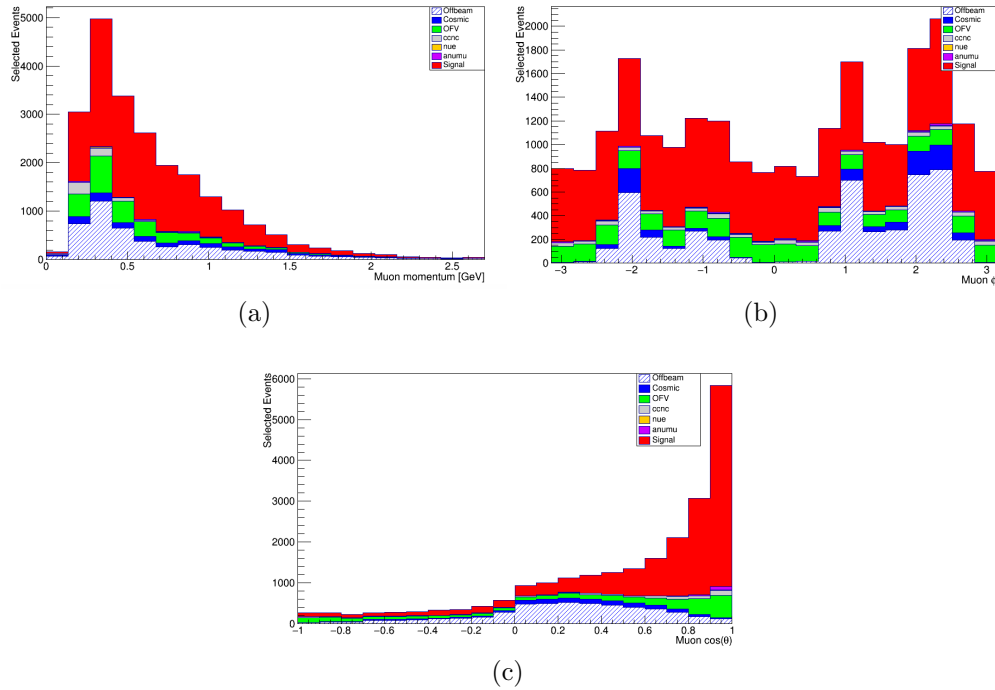


Figure 13: Number of events after the selection and the CRT veto in function of Muon momentum (a), Muon ϕ (b) and Muon $\cos\theta$ (c). The cosmic background is reduced everywhere, and in the ϕ distribution is possible to recognize where the top and the cathode panels are rejecting events.

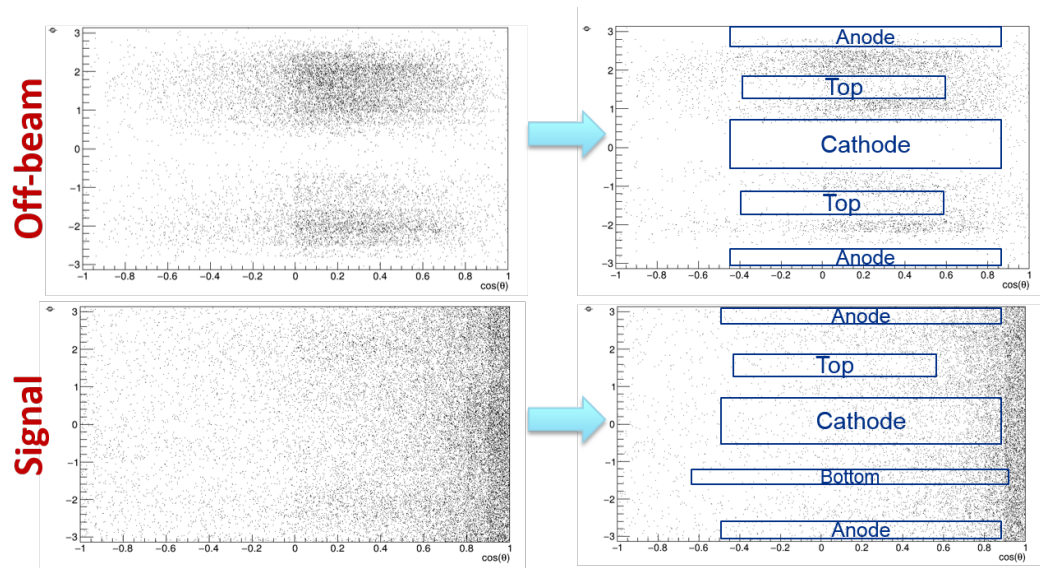


Figure 14: Angular projection ($\cos\theta$ vs ϕ) of selected off-beam and signal particles before and after the CRT veto. The number of tracks is reduced by the panels in the regions shown on the plots on the right.

3 Recovery of lost events in flash matching

In order to try to improve the selection efficiency, is possible to try to recover some events that do not pass the selection. In particular, the flash matching cut reduces the efficiency of 25% (Fig. 3). This cut requires a time matching between the TPC and the PMT information.

	Signal	Cosmic	Off-beam
1 slice	677 (59%)	1187 (7%)	6801 (5%)
More than 1 slice, only one muon not hitting CRT	425 (72%)	278 (20%)	936 (10%)
More than 1 slice, more than one muon not hitting CRT	489 (71%)	408 (18%)	890 (12%)
More than 1 slice, all muons hitting CRT	34 (90%)	820 (23%)	2117 (14%)

Table 3: Number of events that after failing the flash matching can be recovered and pass the quality cuts. Even though only a small part of the total background events are recovered, they are still much more than the recovered signal events.

For the events that don't pass the flash matching cut the CRT were used to reject the muon tracks that hit them. The selected muon candidate in every event has been chosen as the one with the longest projection on the beam axis, because muons coming from neutrino interactions should be forward going. Using all the other quality cuts is possible to recover more than 1000 signal events, but much more background events. So even if the efficiency can be improved, the purity decrease of 12% after this analysis.

4 Time matching

Every neutrino event is on time with the beam spill. Requiring a coincidence between the CRT hit time and the beam spill time, it should be possible to not reject signal events anymore. A better strategy to implement the CRT can be the time matching. It consists in rejecting not all the tracks that hit the CRT, but only the ones that hit the CRT not in time with the beam spill. For this kind of analysis two new simulations for on-beam and off-beam events have been used. In these simulations, true timing information were provided, and it was possible to compare them with the beam spill window. For the off-beam events the window was $[3600-5400]\mu s$, for the other events the window was $[3100-4900]\mu s$.

Timing information could also give a better estimation of the x position of the vertexes. Usually this coordinate is obtained considering the drift velocity of the electrons in the Liquid Argon and their travel time. But as start time in the reconstruction is always used the beam spill initial time, which is clearly different from the true time for a cosmic event. Using timing information from the simulation x positions have been changed properly.

With time matching analysis, considering only the top and the anode panel, it is possible to not reduce the efficiency of the previous selection increasing the purity up to 65.3% (just like the CRT veto selection). The reason why the purity is not bigger than the one from the CRT veto, is that requiring a coincidence does not allow to reject beam induced backgrounds like out of fiducial volume events (they become the 11% of the selected events in this case).

In order to try to improve the results, it is possible to implement CRT as first step of the selection. In particular, for each event, all the muons that are hitting the CRT not in time can be rejected at the beginning of the analysis. With this approach it should be easier to choose the muon coming from the neutrino interaction in every event.

At the end of the selection using only the top and the cathode panel, the purity is 67.3% and the efficiency is slightly reduced (53.6%). But with the simulated cosmic events is possible to use the information about the muon momentum to know if the cosmic muon is stopping inside the liquid argon. Knowing that, cosmic tracks that are not stopping inside the TPC can be extended not only upwards, but also in the other direction. Some of the muons that are passing between the top and the side panel can now be tagged while exiting the cryostat. The results of this selection are better

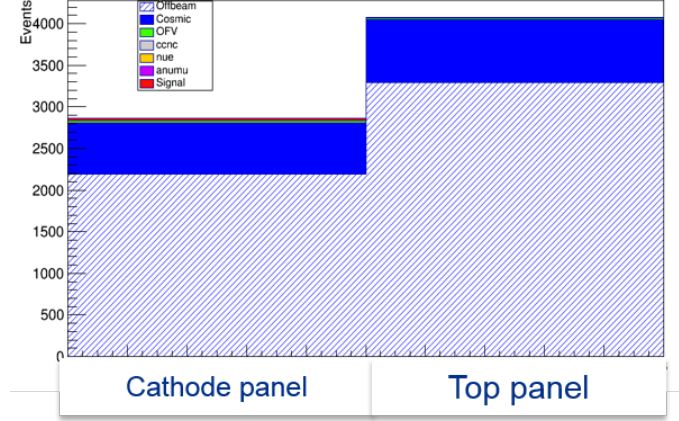


Figure 15: Number of tracks tagged by the top and the cathode panel of the CRT using the time matching.

than the previous, and in this case also the anode and the bottom panels are useful. The number of exiting cosmic tracks tagged by anode and cathode panels is the same, as expected, if the intrinsic difference between the two parts of the detector is taken in account. The efficiency in this case is 53%, but the purity is 71.6%. The cosmic left are the 2% and the off-beam left the 13.9%.

Signal	71.6%
Cosmic	2%
OUTFV	10.1%
CCNC	2.3%
ν_e	0.35%
$\bar{\nu}_\mu$	0.65%
Off-beam	13.9%

Table 4: Event composition after the CRT time matching at the beginning of the selection, using all the panels.

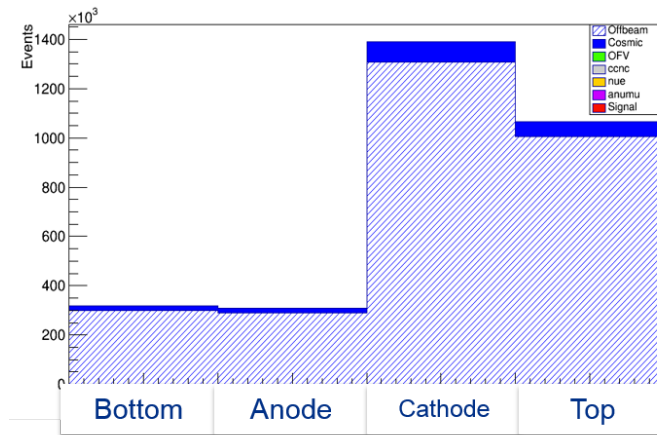


Figure 16: Number of tracks tagged by each panel after extending the cosmic tracks in both directions, implementing the time matching at the beginning of the selection. In this case the cathode panel rejects more events than the top because it can tag both entering and exiting particles.

The background events that are not tagged are the ones that are in time with the beam spill time (it happens often for the off-beam) or the ones that do not hit any panels because of the limited CRT coverage for MicroBooNE.

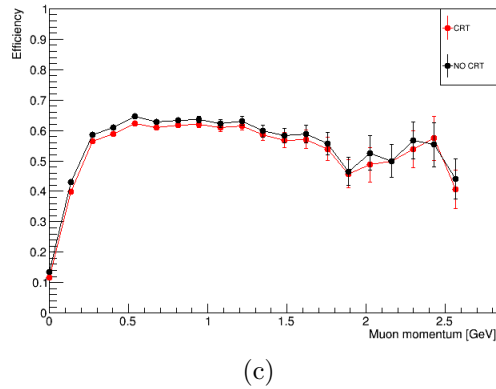
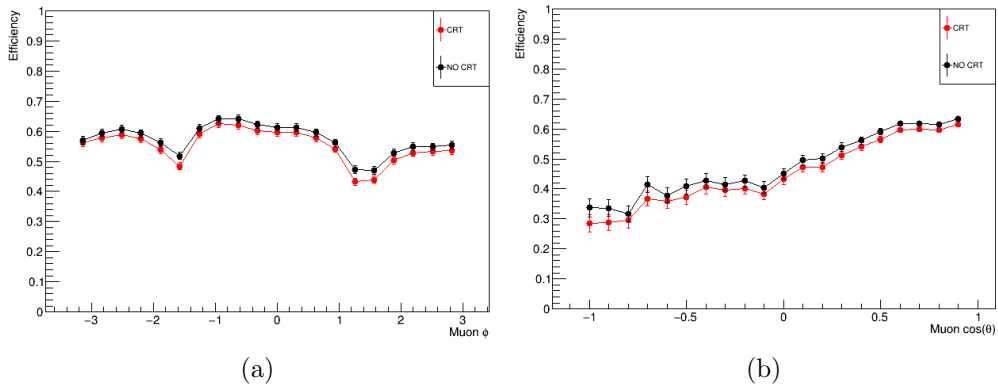


Figure 17: Efficiency of the time matching as first selection step in function of muon ϕ (a), muon $\cos\theta$ (b) and muon momentum (c). The black line is the efficiency of the previous selection, the red one is adding the CRT. The shape of the two lines is exactly the same.

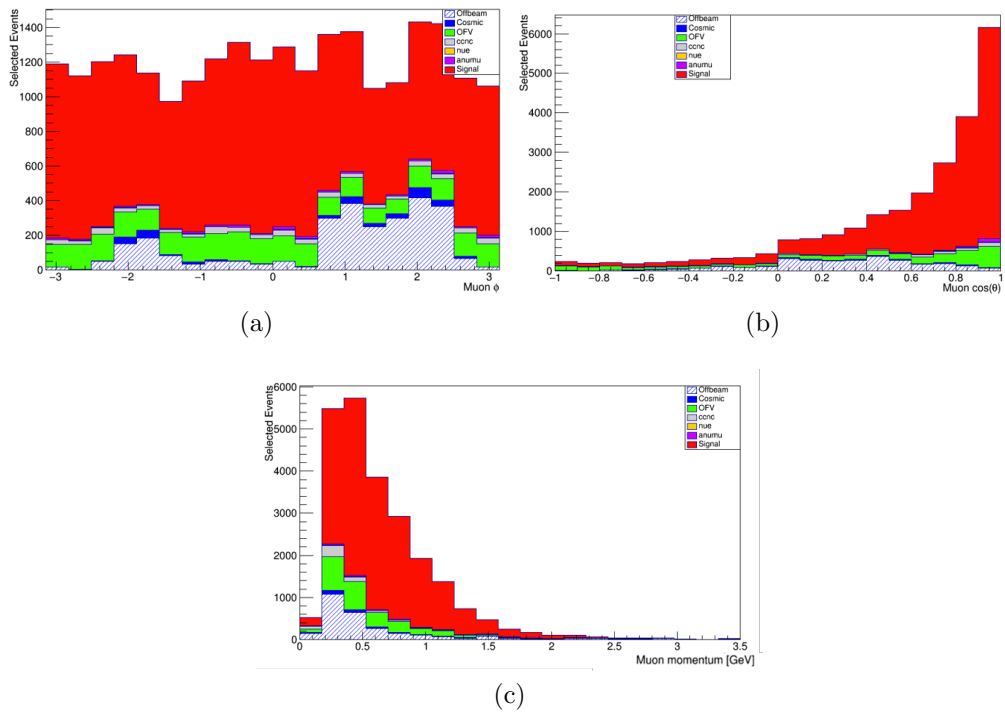


Figure 18: Number of selected events in function of muon ϕ (a), muon $\cos \theta$ (b) and muon momentum (c). The cosmic background is mostly reduced from the previous selection.

5 CRT in future detectors

For SBND and Icarus, there will almost be a 4π CRT coverage.

Considering an hypothetical perfect coverage with 6 panels all around the TPC, background rejection with MicroBooNE data has been studied. With the time matching is possible to reach a 76.1% purity with a 55.2% efficiency. The only cosmic background left are 0.5% cosmic and 8.9% off-beam events. These are the cosmic muons in time with beam spill that can't be rejected using this strategy. Further analysis should be done in order to understand how to reduce beam induced backgrounds, in particular the out of fiducial events, that in this case are the 11.6% of the selected events.

Also in this case the top and the cathode panels tag the same number of events (within statistical uncertainties), while the anode panel is tagging less events. This asymmetry is due to the detector features, because there are more tracks near the cathode than near the anode.

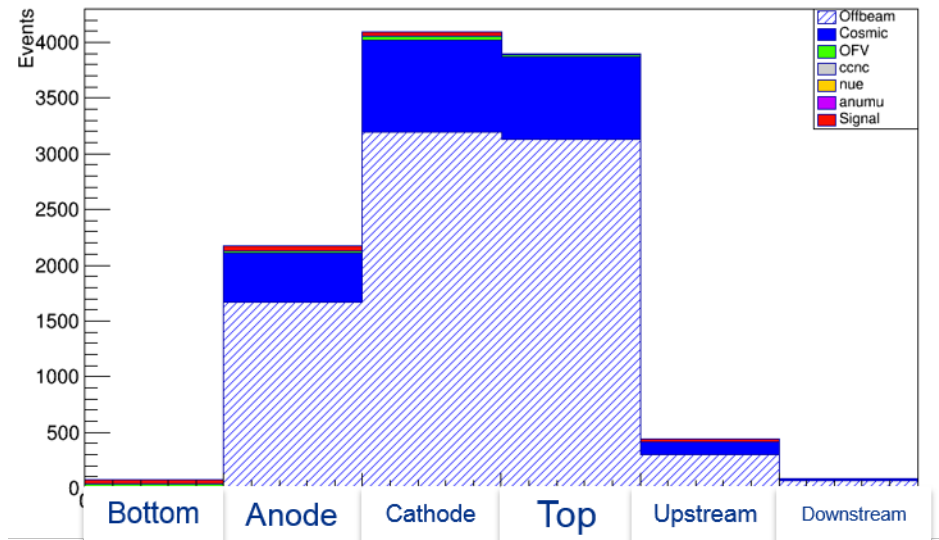


Figure 19: Number of events tagged by each panel considering a full CRT coverage. Double tagging are not shown, so if a particle is hitting two panels, only the first one is in the histogram.

Conclusion

Cosmic background is the main background for the SBN program detectors. MicroBooNE, which is the only detector that is already taking data, has some scintillator panels around the TPC, called Cosmic Ray Tagger (CRT), that can be used to tag and reject the cosmic events. CRT can be used in several ways in order to try to reduce cosmic backgrounds.

Adding a CRT veto, i.e. rejecting all the particles that hit the CRT, is possible to increase the purity of the CC inclusive selection (12%), losing 4% in efficiency. Only two panels, the top and the cathode, are helpful using this strategy.

Considering a time matching, the selection can be improved. All the signal events tagged by CRT can be recovered, restoring the selection efficiency (55.3%). Using the time matching at the beginning of the selection and considering now true information of the cosmic tracks, is possible to improve the purity to 71.6%.

On the contrary, CRT information can't be used efficiently to recover signal events that do not pass the flash matching cut, because the majority of the those events are cosmic backgrounds.

Finally, analysis have shown that a full CRT coverage can reject most of the cosmic background, but some ideas need to be developed to reduce beam induced backgrounds like the out of fiducial volume events.

Appendix

Here is provided the list of functions used to determine if a track was hitting a CRT panel or not. The functions for cosmic tracks extend them only upwards. The last function determine how much does a track travel before exiting the cryostat.

The arguments of the functions are the vertex coordinates and the two angles of the track.

```
bool PassTop(Double_t x, Double_t y, Double_t z,
             Double_t theta, Double_t phi)
{
    Double_t dist=(659.5-y)/(sin(theta)*sin(phi));
    bool temp=false;
    if(dist>0){
        Double_t cz=z+dist*cos(theta);
        Double_t cx=x+dist*sin(theta)*cos(phi);
        if((cz<1180. && cz>640. && cx<311.5 && cx>-238.9) ||
          (cz<640.&& cz>460. && cx<490. && cx>-238.9) ||
          (cz<460. && cz>100. && cx<490. && cx>-54.4) ||
          (cz<100.&& cz>-80 && cx<309. && cx>125.9)) temp=true;
    }
    return temp;
}

bool PassTop_cosmic(Double_t x, Double_t y, Double_t z,
                    Double_t theta, Double_t phi)
{
    Double_t dist=(659.5-y)/(sin(theta)*sin(phi));
    Double_t cz=z+dist*cos(theta);
    Double_t cx=x+dist*sin(theta)*cos(phi);
    bool temp=false;
    if((cz<1180. && cz>640. && cx<311.5 && cx>-238.9) ||
      (cz<640.&& cz>460. && cx<490. && cx>-238.9) ||
      (cz<460. && cz>100. && cx<490. && cx>-54.4) ||
      (cz<100.&& cz>-80 && cx<309. && cx>125.9)) temp=true;

    return temp;
}

bool PassCathode(Double_t x, Double_t y, Double_t z,
                  Double_t theta, Double_t phi)
{
    Double_t dist=(378.016-x)/(sin(theta)*cos(phi));
    Double_t dist1=(388.016-x)/(sin(theta)*cos(phi));
}
```



```

bool temp=false;
if(dist>0) {
    Double_t cz=z+dist*cos(theta);
    Double_t cy=y+dist*sin(theta)*sin(phi);
    if(cz<1130.7 && cz>-89.9 &&
        cy<291.486 && cy>31.886){
        temp=true;}
    }

if(dist1>0){
    Double_t cz=z+dist1*cos(theta);
    Double_t cy=y+dist1*sin(theta)*sin(phi);
    if(cz<1130.7 && cz>-89.9 &&
        cy<41.05 && cy>-218.514) {
    temp=true;}
    }

return temp;
}

bool PassCathode_cosmic(Double_t x, Double_t y, Double_t z,
    Double_t theta, Double_t phi)
{
    Double_t dist=(378.016-x)/(sin(theta)*cos(phi));
    Double_t dist1=(388.016-x)/(sin(theta)*cos(phi));

    Double_t cz=z+dist*cos(theta);
    Double_t cy=y+dist*sin(theta)*sin(phi);
    Double_t cz1=z+dist1*cos(theta);
    Double_t cy1=y+dist1*sin(theta)*sin(phi);

    bool temp= false;

    if((cy-y)>0){
        if ((cz<1130.7 && cz>-89.9 &&
            cy<291.486 && cy>31.886))}
        temp=true;}
    }

    if ((cy1-y)>0){
        if(cz1<1130.7 && cz1>-89.9 &&
            cy1<41.05 && cy1>-218.514){
            temp=true;}
        }
}

```

```

    return temp;
}

bool PassAnode(Double_t x, Double_t y, Double_t z,
               Double_t theta, Double_t phi)
{
    Double_t dist=(-136.984-x)/(sin(theta)*cos(phi));
    bool temp=false;
    if(dist>0) {
        Double_t cz=z+dist*cos(theta);
        Double_t cy=y+dist*sin(theta)*sin(phi);
        if(cz<1131.3 && cz>-89.3 &&
           cy<127.514 && cy>-218.514){
            temp=true;}
    }

    return temp;
}

bool PassAnode_cosmic(Double_t x, Double_t y, Double_t z,
                      Double_t theta, Double_t phi)
{
    Double_t dist=(-136.984-x)/(sin(theta)*cos(phi));
    bool temp=false;
    if(dist>0) {
        Double_t cz=z+dist*cos(theta);
        Double_t cy=y+dist*sin(theta)*sin(phi);
        if((cy-y)>0){
            if(cz<1131.3 && cz>-89.3 &&
               cy<127.514 && cy>-218.514){
                temp=true;}
            }
    }

    return temp;
}

bool PassBottom(Double_t x, Double_t y, Double_t z,
                 Double_t theta, Double_t phi)
{

```

```

Double_t dist=(-263.356-y)/(sin(theta)*sin(phi));
Double_t dist1=(-259.856-y)/(sin(theta)*sin(phi));
bool temp=false;
if(dist>0){
    Double_t cz=z+dist*cos(theta);
    Double_t cx=x+dist*sin(theta)*cos(phi);
    if(cz<628.952 && cz>283.342
        && cx<389.616 && cx>-134.384) {
temp=true;}
    }

    if ( dist1>0) {
    Double_t cz=z+dist*cos(theta);
    Double_t cx=x+dist*sin(theta)*cos(phi);
    if(cz<628.952 && cz>283.342
        && cx<389.616 && cx>-134.384) {
temp=true;
    }
    }

    return temp;
}
}

double Range(Double_t nx, Double_t ny, Double_t nz,
    Double_t th, Double_t ph ){

double z1=-24.745;
double z2=1061.74;
double r=191.61;
double xcenter=128.175;

double l, dist_cyl, tr_range, aus1, aus2, rplus, cx, cy, cz;
l=dist_cyl=tr_range=aus1=aus2=rplus=cz=cy=cx=0;

dist_cyl=(z1-nz)/cos(th);
cx=nx+dist_cyl*sin(th)*cos(ph);
cy=ny+dist_cyl*sin(th)*sin(ph);
if(dist_cyl>0 && (cy*cy+(cx-xcenter)*(cx-xcenter))<(r*r)) {
    l=dist_cyl;
}
}

```

```

cx=cz=cy=0;

dist_cyl=(z2-nz)/cos(th);
cx=nx+dist_cyl*sin(th)*cos(ph);
cy=ny+dist_cyl*sin(th)*sin(ph);
if(dist_cyl>0 && (cy*cy+(cx-xcenter)*(cx-xcenter))<(r*r)) {
    l=dist_cyl;
}

cx=cy=cz=0;

if(l==0) {

    aus1=(nx-xcenter)*cos(ph)+ny*sin(ph);
    aus2=(nx-xcenter)*(nx-xcenter)+ny*ny-r*r;

    rplus=aus1+sqrt(aus1*aus1-aus2);

    l=rplus/sin(th);
}

return l;
}
}

```

References

- [1] *Proposal for a Three Detector Short-Baseline Neutrino Oscillation Program in the Fermilab Booster Neutrino Beam*, 2015, arXiv:1503.01520
- [2] M. Auger, I. Kreslo and D. L. Galindo, *MicroBooNE CRT design and performance Technical Note*, 2016
- [3] The MicroBooNE collaboration *Design and Construction of the MicroBooNE Detector*, 2016, arXiv:1612.05824
- [4] The MicroBooNE Collaboration, *MicroBooNE Public Note MICROBOONE-NOTE-1045-PUB*; <http://microboone.fnal.gov/wp-content/uploads/MICROBOONE-NOTE-1045-PUB.pdf>, 2018
- [5] PDG 2017, http://pdg.lbl.gov/2017/AtomicNuclearProperties/MUE/muE_liquid_argon.pdf